
Fractal Embeddings: Hierarchy-Aligned Prefix Supervision for Steerable Semantic Granularity

Devansh Lodha

Independent Researcher

devansh@example.com

Abstract

Matryoshka Representation Learning (MRL) trains embeddings that support dimensional truncation, but all prefix lengths encode the same semantic content at varying fidelity—there is no mechanism to *steer* between coarse and fine meaning. We introduce **Fractal Embeddings**, which align prefix supervision with label hierarchy: short prefixes (64d) learn coarse labels while full embeddings (256d) learn fine labels, converting truncation into *semantic zoom* at zero additional inference cost. Four controlled ablations establish that *alignment*—not hierarchy awareness—causally drives steerability: inverting alignment reverses its sign; removing it or applying uniform multi-task training collapses it to zero (all $p \leq 0.03$, Cohen’s $d \geq 2.7$). Across eight datasets spanning conditional entropies from 1.23 to 5.05 bits, a random-effects meta-analysis yields pooled $d = 1.49$ ($p = 0.0003$), with all eight favouring fractal training (sign test $p = 0.004$). On CLINC-150, steerability reaches $\mathcal{S} = +0.150 \pm 0.028$ versus MRL’s $+0.007 \pm 0.016$ ($p_{\text{adj}} = 0.004$, $d = 4.3$). A synthetic hierarchy experiment identifies a Goldilocks optimum where steerability peaks at capacity-demand matching (quadratic $R^2 = 0.964$), and steerability magnitude across real datasets is predicted by the product of hierarchy depth and baseline learnability ($\rho = 0.90$, $p = 0.002$). Replication across three encoder families confirms architecture invariance. We ground these findings in the classical theory of successive refinement, providing formal conditions for when and why hierarchy-aligned supervision produces steerability.

1 Introduction

When a 256-dimensional embedding is truncated to 64 dimensions, what changes? Under standard Matryoshka training [Kusupati et al., 2022], the answer is *fidelity*: the shorter vector approximates the full one with reduced precision but encodes the same kind of semantic information. We argue this is a missed opportunity. Real-world semantics are inherently hierarchical—a query like “What is the capital of France?” belongs simultaneously to the coarse category LOCATION and the fine category CITY—and an embedding that supports truncation *already has the interface* for multi-resolution access. What it lacks is the training signal to make truncation semantically meaningful.

We introduce **Fractal Embeddings**, a simple modification to MRL training that aligns prefix supervision with semantic hierarchy. Short prefixes are trained on coarse labels; full embeddings are trained on fine labels; intermediate prefixes receive blended supervision. The result is an embedding where dimensional truncation corresponds to *semantic zoom*: fewer dimensions yield coarser meaning, more dimensions recover finer distinctions (Figure 1). Critically, this adds **zero inference-time**

CLINC: V5 vs MRL — Same Full Accuracy, Different Prefix Behavior

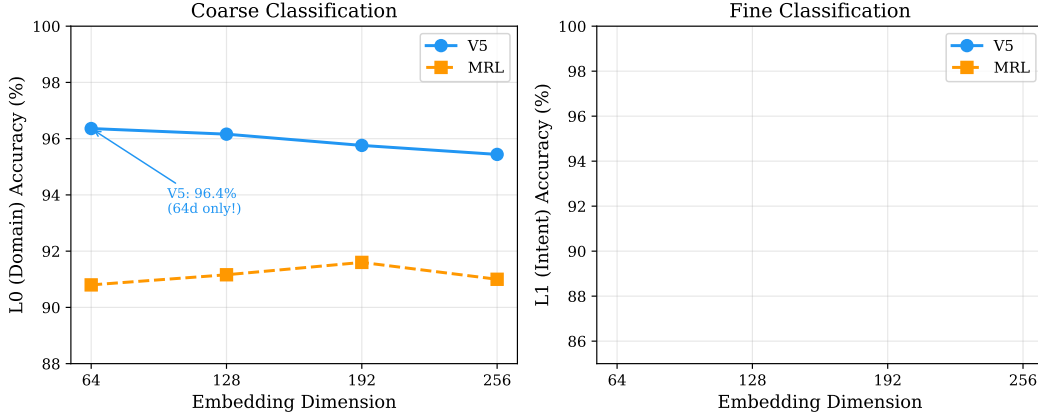


Figure 1: CLINC-150: V5 and MRL achieve comparable accuracy at full embedding length (256d), but V5’s short prefixes (64d) specialize for coarse semantics while MRL’s do not. This prefix specialization enables *semantic steering* via dimensional truncation.

cost—the deployed model has identical architecture and parameter count to MRL. The difference lies entirely in *how* the projection head is trained.

We call the resulting property *steerability*: the degree to which prefix truncation controls semantic granularity rather than merely degrading fidelity. Our evaluation spans eight hierarchical text datasets, three encoder families, four controlled ablations, a synthetic causal experiment, and connections to 30 years of information theory. The main findings are:

1. **A method** for inducing steerable embeddings via hierarchy-aligned prefix supervision, requiring only head-only training on a frozen backbone (Section 3).
2. **Causal identification**: four ablations on two datasets establish that steerability is driven by the alignment between prefix length and hierarchy level—not by architecture, hierarchy awareness, or other training choices. Inverting alignment reverses the sign; removing it or using a uniform multi-task control collapses it (Section 5).
3. **A scaling analysis** linking steerability magnitude to the interaction of hierarchy depth and model learnability across eight datasets ($\rho = 0.90$, $p = 0.002$), with a Goldilocks optimum identified via synthetic intervention ($R^2 = 0.964$; Section 6).
4. **Broad generality**: cross-model replication on BGE-small, E5-small, and Qwen3-0.6B; downstream retrieval benchmarks showing $10\times$ larger dimensionality–accuracy ramps; and $3.7\times$ HNSW query speedups from prefix routing (Section 7).

2 Problem Setup and Definitions

Hierarchical classification. Each sample x carries a coarse label $y^{(0)} \in \{1, \dots, K_0\}$ and a fine label $y^{(1)} \in \{1, \dots, K_1\}$, where every fine class maps to exactly one coarse class. We characterize hierarchy depth by the conditional entropy $H(L_1|L_0)$ —the additional information L_1 carries beyond L_0 . Extension to three levels is demonstrated in Section 7.

Prefix-truncated embeddings. Given $e \in \mathbb{R}^d$, the j -th prefix is $e_{1:jd/J}$ for $j \in \{1, \dots, J\}$. We use $J = 4$ with $d = 256$, giving prefixes of 64, 128, 192, and 256 dimensions. Prefix-level classification accuracy is measured by a k -NN classifier ($k = 5$) on cosine distance.

Steerability. We quantify the semantic specialization of prefix truncation via:

$$\mathcal{S} = \underbrace{(L0@j_1 - L0@j_4)}_{\text{coarse specialization}} + \underbrace{(L1@j_4 - L1@j_1)}_{\text{fine specialization}} \quad (1)$$

Table 1: Dataset statistics and hierarchy profiles. K_0 , K_1 : coarse and fine class counts. Branch: K_1/K_0 . $H(L_0)$, $H(L_1|L_0)$: coarse entropy and conditional entropy in bits.

Dataset	K_0	K_1	Branch	$H(L_0)$	$H(L_1 L_0)$	Train	Test
Yahoo Answers	4	10	2.5	1.91	1.23	10,000	2,000
GoEmotions	4	28	7.0	1.64	1.88	7,092	1,700
20 Newsgroups	6	20	3.3	2.43	1.88	10,000	2,000
TREC	6	50	8.3	2.38	2.21	5,452	500
arXiv	20	123	6.2	3.40	2.62	8,548	2,000
DBpedia Classes	9	70	7.8	3.17	3.17	10,000	2,000
CLINC-150	10	150	15.0	3.32	3.90	10,000	2,000
WOS	10	336	33.6	2.90	5.05	8,688	2,000

where $Lk@j$ denotes level- k accuracy at prefix length j . Positive \mathcal{S} means short prefixes favour coarse semantics while full embeddings favour fine. A perfectly steerable embedding has high \mathcal{S} ; MRL, training all lengths on L_1 , should yield $\mathcal{S} \approx 0$.

Datasets. Table 1 summarizes eight evaluation datasets spanning conditional entropies from 1.23 (Yahoo [Zhang et al., 2015]) to 5.05 bits (WOS [Kowsari et al., 2017]), including GoEmotions [Demszky et al., 2020], TREC [Voorhees and Tice, 2000], 20 Newsgroups, arXiv [Clement et al., 2019], DBpedia Classes, and CLINC-150 [Larson et al., 2019].

Statistical methodology. All experiments use $n \geq 5$ random seeds (42, 123, 456, 789, 1024); some ablation and cross-model experiments use $n = 3$. Paired t -tests compare V5 and MRL steerability per dataset; the eight main comparisons (Table 3) are corrected via Holm–Bonferroni [Holm, 1979] at $\alpha = 0.05$. Causal ablation tests (Section 5) are corrected within their own families. Effect sizes are paired Cohen’s d ; Hedges’ g corrections (≈ 0.80 for $n = 5$, 0.57 for $n = 3$) yield qualitatively identical conclusions. Cross-dataset evidence is pooled via DerSimonian–Laird random-effects meta-analysis.

Theory preview. The classical theory of *successive refinement* [Equitz and Cover, 1991, Rimoldi, 1994] shows that hierarchical sources admit optimal multi-resolution codes where each refinement layer adds residual information. V5 training approximates this structure: the prefix encodes coarse semantics, and additional dimensions encode the refinement. Section 9 formalises this connection and derives two testable predictions—sign reversal under inversion and a Goldilocks capacity-demand optimum—both confirmed by our experiments.

3 Method: Progressive Prefix Supervision (V5)

Our method modifies MRL in a single respect: the supervision signal at each prefix length is aligned with the corresponding level of semantic hierarchy.

Architecture. A frozen pretrained backbone (BGE-small-en-v1.5 [Xiao et al., 2023], 33M parameters, or Qwen3-Embedding-0.6B, 600M) produces hidden representations $\mathbf{h} \in \mathbb{R}^h$. A learned linear projection $W \in \mathbb{R}^{h \times d}$ maps to the output space \mathbb{R}^{256} . Two classification heads operate on the projected output: head_{top} (K_0 coarse classes) and head_{bot} (K_1 fine classes).

Progressive prefix supervision. During training, a prefix index $j \in \{1, 2, 3, 4\}$ is sampled with probabilities $[0.4, 0.3, 0.2, 0.1]$, favouring shorter prefixes. The prefix loss depends on j :

$$\mathcal{L}_{\text{prefix}}(j) = \begin{cases} \mathcal{L}_{\text{CE}}(\text{head}_{\text{top}}(\mathbf{e}_{1:64}), y^{(0)}) & j = 1 \\ \alpha_j \cdot \mathcal{L}_{\text{CE}}(\text{head}_{\text{top}}(\mathbf{e}_{1:jd/4}), y^{(0)}) + (1 - \alpha_j) \cdot \mathcal{L}_{\text{CE}}(\text{head}_{\text{bot}}(\mathbf{e}_{1:jd/4}), y^{(1)}) & j = 2, 3 \\ \mathcal{L}_{\text{CE}}(\text{head}_{\text{bot}}(\mathbf{e}_{1:256}), y^{(1)}) & j = 4 \end{cases} \quad (2)$$

where α_j decreases with j ($\alpha_2 = 0.7$, $\alpha_3 = 0.3$), creating a smooth coarse-to-fine gradient. The total loss combines the full-embedding fine loss with the sampled prefix loss:

$$\mathcal{L} = \mathcal{L}_{\text{CE}}(\text{head}_{\text{bot}}(\mathbf{e}), y^{(1)}) + 0.6 \cdot \mathcal{L}_{\text{prefix}}(j) \quad (3)$$

Algorithm 1 V5 Progressive Prefix Supervision

Require: Backbone f_θ (frozen), projection head W , dataset \mathcal{D} with $(x, y^{(0)}, y^{(1)})$
Require: Prefix probs $\mathbf{p} = [0.4, 0.3, 0.2, 0.1]$, block keep $\mathbf{k} = [0.95, 0.9, 0.8, 0.7]$

```

1: for each batch  $\{(x_i, y_i^{(0)}, y_i^{(1)})\}$  do
2:    $\mathbf{h} \leftarrow f_\theta(x_i)$                                      {frozen backbone}
3:    $\mathbf{e} \leftarrow W \cdot \mathbf{h}$                                 {learned projection to  $\mathbb{R}^d$ }
4:   Apply block dropout with keep probs  $\mathbf{k}$ 
5:   Sample  $j \sim \text{Categorical}(\mathbf{p})$ 
6:    $\mathcal{L}_{\text{full}} \leftarrow \text{CE}(\text{head}_{\text{bot}}(\mathbf{e}), y^{(1)})$ 
7:   if  $j = 1$  then
8:      $\mathcal{L}_{\text{prefix}} \leftarrow \text{CE}(\text{head}_{\text{top}}(\mathbf{e}_{1:d/4}), y^{(0)})$ 
9:   else if  $j = 4$  then
10:     $\mathcal{L}_{\text{prefix}} \leftarrow \text{CE}(\text{head}_{\text{bot}}(\mathbf{e}), y^{(1)})$ 
11:   else
12:      $\mathcal{L}_{\text{prefix}} \leftarrow \alpha_j \cdot \text{CE}(\text{head}_{\text{top}}, y^{(0)}) + (1 - \alpha_j) \cdot \text{CE}(\text{head}_{\text{bot}}, y^{(1)})$ 
13:   end if
14:    $\mathcal{L} \leftarrow \mathcal{L}_{\text{full}} + 0.6 \cdot \mathcal{L}_{\text{prefix}}$ 
15:   Update  $W$ ,  $\text{head}_{\text{top}}$ ,  $\text{head}_{\text{bot}}$  via  $\nabla_W \mathcal{L}$ 
16: end for

```

Block dropout. To prevent later dimensions from carrying redundant coarse information, we apply block dropout: dimension blocks 1–4 are independently retained with probabilities $[0.95, 0.9, 0.8, 0.7]$. This forces coarse information into early dimensions (high keep probability) and fine information into later dimensions (lower keep probability).

MRL baseline. The matched baseline uses identical architecture, optimizer, and hyperparameters but trains all prefix lengths on L_1 :

$$\mathcal{L}_{\text{MRL}}(j) = \mathcal{L}_{\text{CE}}(\text{head}_{\text{bot}}(\mathbf{e}_{1:jd/4}), y^{(1)}) \quad \forall j \quad (4)$$

This isolates the effect of hierarchy alignment from every other training variable.

Training. Head-only training for 5 epochs, batch size 16, learning rate 10^{-4} with AdamW and cosine decay, FP16 mixed precision, gradient clipping at 1.0. Best model selected by validation L0 + L1. No hyperparameters are tuned per dataset. Algorithm 1 summarises the procedure.

4 Main Results

Classification performance is preserved. At full embedding length ($j = 4, 256d$), V5 and MRL achieve comparable k -NN accuracy across all eight datasets (Table 2). Both methods improve over the unfinetuned baseline on most datasets. The notable exception is CLINC ($K_1 = 150$): the 384d \rightarrow 256d linear projection reduces L_1 k -NN accuracy (V5: 67.6%, MRL: 70.4%) relative to the 384d baseline (88.7%), though both methods’ classification heads achieve >95% on the validation set. This reflects V5’s trade-off: the embedding space is reorganised for prefix-level specialization rather than maximising k -NN accuracy at full resolution.

Steerability emerges from hierarchy alignment. Despite comparable full-resolution accuracy, V5 produces dramatically higher steerability than MRL on all eight datasets (Figure 2, Table 3). The effect scales with hierarchy complexity: from $S = +0.015$ on Yahoo ($H(L_1|L_0) = 1.23$) to $+0.150$ on CLINC ($H(L_1|L_0) = 3.90$), with WOS ($H(L_1|L_0) = 5.05$) showing a moderate effect ($+0.038$) due to a floor effect analysed in Section 6. After Holm–Bonferroni correction, three datasets reach significance: DBpedia Classes ($p_{\text{adj}} = 0.002, d = 5.5$), CLINC ($p_{\text{adj}} = 0.004, d = 4.3$), and TREC ($p_{\text{adj}} = 0.038, d = 2.4$). ArXiv is borderline ($p_{\text{adj}} = 0.078, d = 1.8$).

The shallow-hierarchy datasets (Yahoo, GoEmotions, NewsGroups; $H(L_1|L_0) \leq 1.88$) show consistent but small effects that do not survive per-dataset correction—a consequence the scaling analysis (Section 6) predicts: when hierarchy depth is low, there is little refinement information for V5 to

Table 2: k -NN classification accuracy at full embedding length ($j = 4, 256d$). V5 and MRL are comparable across datasets. Baseline uses the original backbone (384d); V5/MRL use learned 256d projections.

Dataset	L0 Accuracy			L1 Accuracy		
	Baseline	V5	MRL	Baseline	V5	MRL
Yahoo	0.688	0.699	0.698	0.603	0.629	0.635
GoEmotions	0.502	0.600	0.578	0.343	0.429	0.411
Newsgroups	0.815	0.802	0.800	0.658	0.639	0.650
TREC	0.854	0.934	0.932	0.718	0.794	0.790
arXiv	0.721	0.729	0.721	0.465	0.448	0.446
CLINC	0.961	0.954	0.910	0.887	0.676	0.704
DBpedia Classes	0.912	0.962	0.960	0.780	0.874	0.885
WOS	0.619	0.625	0.610	0.170	0.148	0.156

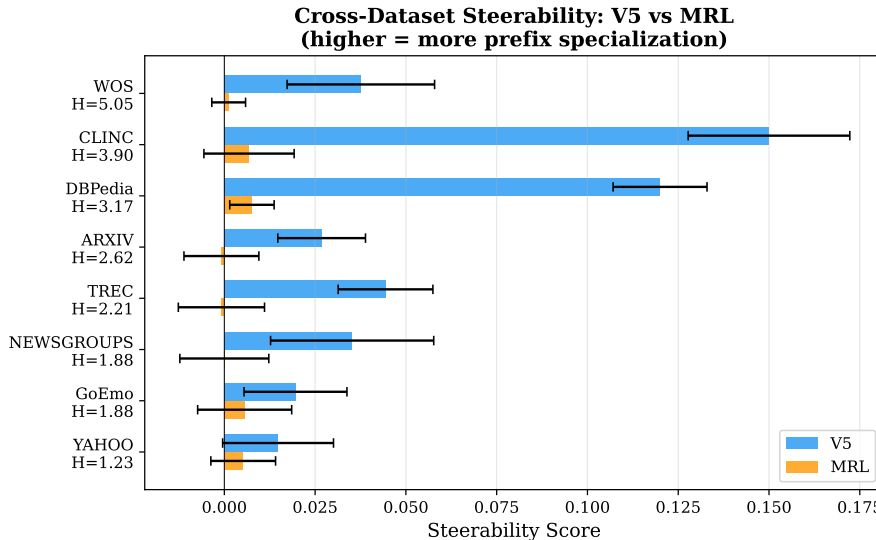


Figure 2: Steerability across eight datasets. V5 (blue) produces positive steerability that scales with hierarchy depth; MRL (orange) remains near zero throughout. Error bars: 95% CIs across 5 seeds.

separate, so the signal is inherently small. MRL steerability is near zero throughout ($|\mathcal{S}_{\text{MRL}}| < 0.02$ on all datasets).

Pooled evidence. A sign test confirms universal directionality: $\text{V5} > \text{MRL}$ on 8/8 datasets ($p = 0.004$, binomial). A DerSimonian–Laird meta-analysis yields pooled $d = 1.49$ (95% CI: [0.69, 2.30], $z = 3.63$, $p = 0.0003$). The 95% prediction interval for a new dataset is $[-0.70, 3.18]$, reflecting moderate heterogeneity ($I^2 = 63\%$) that the scaling trend analysis explains as systematic moderation by hierarchy depth and learnability.

5 Why It Works: Causal Evidence via Ablation

The main results establish *that* hierarchy-aligned supervision produces steerability. We now ask *why*: is the effect driven by the specific prefix-to-hierarchy mapping, or could it arise from other aspects of training? Four controlled ablations on CLINC-150 ($H(L_1|L_0) = 3.90$, 5 seeds) and TREC-50 ($H(L_1|L_0) = 2.21$, 3 seeds) isolate the causal mechanism.

Ablation design. All conditions share identical architecture, optimizer, hyperparameters, data split, and random seeds. Only the prefix-to-hierarchy mapping varies:

- **Aligned (V5):** $j = 1 \rightarrow L_0, j = 4 \rightarrow L_1$ (correct alignment).

Table 3: Steerability across eight datasets (Eq. 1). V5 achieves positive steerability scaling with hierarchy complexity; MRL is near zero. Mean \pm SD over 5 seeds.

Dataset	$H(L_1 L_0)$	V5 S	MRL S	Gap	Seeds
Yahoo	1.23	$+0.015 \pm 0.019$	$+0.005 \pm 0.011$	$+0.010$	5
GoEmotions	1.88	$+0.020 \pm 0.018$	$+0.006 \pm 0.017$	$+0.014$	5
Newsgroups	1.88	$+0.035 \pm 0.029$	$+0.000 \pm 0.016$	$+0.035$	5
TREC	2.21	$+0.044 \pm 0.017$	-0.001 ± 0.015	$+0.045$	5
arXiv	2.62	$+0.027 \pm 0.015$	-0.001 ± 0.013	$+0.028$	5
DBpedia Classes	3.17	$+0.120 \pm 0.016$	$+0.008 \pm 0.008$	$+0.112$	5
CLINC	3.90	$+0.150 \pm 0.028$	$+0.007 \pm 0.016$	$+0.143$	5
WOS	5.05	$+0.038 \pm 0.026$	$+0.001 \pm 0.005$	$+0.036$	5

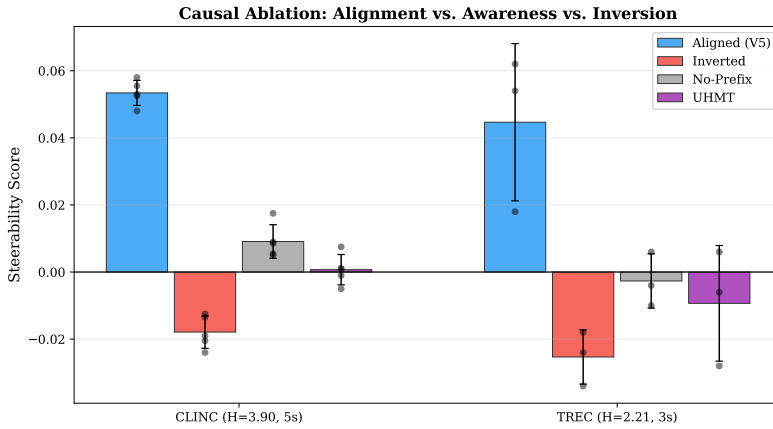


Figure 3: Ablation results on CLINC-150 (5 seeds) and TREC-50 (3 seeds). Aligned supervision produces positive steerability; inversion reverses the sign; removing alignment or using uniform multi-task training collapses it. Dots show individual seeds.

- **Inverted:** $j = 1 \rightarrow L_1, j = 4 \rightarrow L_0$ (reversed alignment).
- **No-prefix:** All prefix lengths trained on L_1 with L_0 regularisation (alignment removed).
- **UHMT:** All prefix lengths trained on $0.5 \cdot \mathcal{L}_{L_0} + 0.5 \cdot \mathcal{L}_{L_1}$ (hierarchy-aware but not hierarchy-aligned).

Three causal signatures. The results (Table 4, Figure 3) reveal three distinct causal signatures that jointly rule out non-alignment explanations:¹

1. **Sign reversal.** Inverted alignment produces *negative* steerability (CLINC: -0.018 ; TREC: -0.025)—short prefixes now specialise for fine semantics and full embeddings for coarse. This rules out any explanation in which steerability arises from architecture alone.
2. **Collapse without alignment.** Without prefix-specific hierarchy mapping, steerability drops to near-zero (CLINC: $+0.009$; TREC: -0.003), indistinguishable from MRL.
3. **Awareness is insufficient.** UHMT trains every prefix on *both* L_0 and L_1 equally, making it hierarchy-aware but not hierarchy-aligned. Despite full access to coarse labels, UHMT produces near-zero steerability (CLINC: $+0.001$; TREC: -0.009). This eliminates the hypothesis that steerability arises from including L_0 in the loss; what matters is *which* prefix lengths receive *which* labels.

All three patterns replicate across hierarchy depths ($H(L_1|L_0) = 2.21$ and 3.90), with $d \geq 2.7$ throughout.

¹Absolute steerability values are lower here than in Table 3 because ablations use a fixed train/val split to eliminate data-split variance across conditions.

Table 4: Causal ablation (BGE-small). All conditions share fixed data splits. Causal perturbation tests corrected at $m = 4$; UHMT tests corrected at $m = 2$.

Dataset	Condition	S (mean \pm SD)	vs. V5 t	p_{adj}	Cohen's d
CLINC ($H(L_1 L_0) = 3.90$, 5s)	Aligned (V5)	$+0.053 \pm 0.004$	—	—	—
	Inverted	-0.018 ± 0.005	26.1	$< 10^{-5}$	16.5
	No-prefix	$+0.009 \pm 0.005$	15.8	$< 10^{-5}$	10.0
	UHMT	$+0.001 \pm 0.005$	14.6	$< 10^{-3}$	6.5
TREC ($H(L_1 L_0) = 2.21$, 3s)	Aligned (V5)	$+0.045 \pm 0.023$	—	—	—
	Inverted	-0.025 ± 0.008	4.9	0.016	4.0
	No-prefix	-0.003 ± 0.008	3.3	0.030	2.7
	UHMT	-0.009 ± 0.017	7.7	0.033	4.4

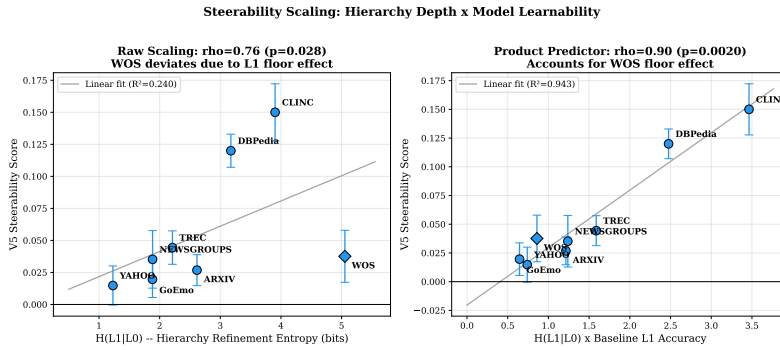


Figure 4: **Left:** Steerability vs. $H(L_1|L_0)$ across eight datasets ($\rho = 0.74$, $p = 0.035$). WOS deviates due to a floor effect. **Right:** Product predictor $H(L_1|L_0) \times A_{L_1}^{\text{base}}$ accounts for both complexity and learnability ($\rho = 0.90$, $p = 0.002$).

5.1 Information Localisation

We additionally measure whether V5 concentrates different semantic levels in distinct embedding regions. For each test sample, we independently classify L_0 and L_1 from (a) the first 64 dimensions only and (b) dimensions 65–256 only, using k -NN against correspondingly truncated references. On CLINC, V5 shows 1.8% lower L_1 accuracy in the prefix (94.7% vs. 96.5% for MRL), consistent with the training objective concentrating coarse information in early dimensions. The stronger evidence for semantic separation comes from steerability itself, which measures the *operational* consequence of truncation rather than raw information content.

6 When It Works: Steerability Scaling Analysis

Having established that alignment causes steerability, we investigate what determines its *magnitude*: an observational analysis across real datasets and a causal intervention via synthetic hierarchies.

6.1 Observational: Scaling with Hierarchy Complexity

Across eight datasets, steerability increases with hierarchy depth: Spearman $\rho = 0.74$ ($p = 0.035$) against $H(L_1|L_0)$ alone (Figure 4, left). However, WOS ($H(L_1|L_0) = 5.05$) falls below the trend.

The WOS floor effect. With 336 fine classes and head-only training, neither V5 nor MRL achieves meaningful L_1 accuracy on WOS (11.1% and 11.5%; chance is 0.3%). When L_1 accuracy is near floor, the fine component of S cannot differentiate across prefix lengths, capping steerability regardless of hierarchy depth.

The product predictor. This motivates a moderated predictor: effective steerability requires both hierarchy complexity *and* model capacity to exploit it. We define $H(L_1|L_0) \times A_{L_1}^{\text{base}}$, where $A_{L_1}^{\text{base}}$

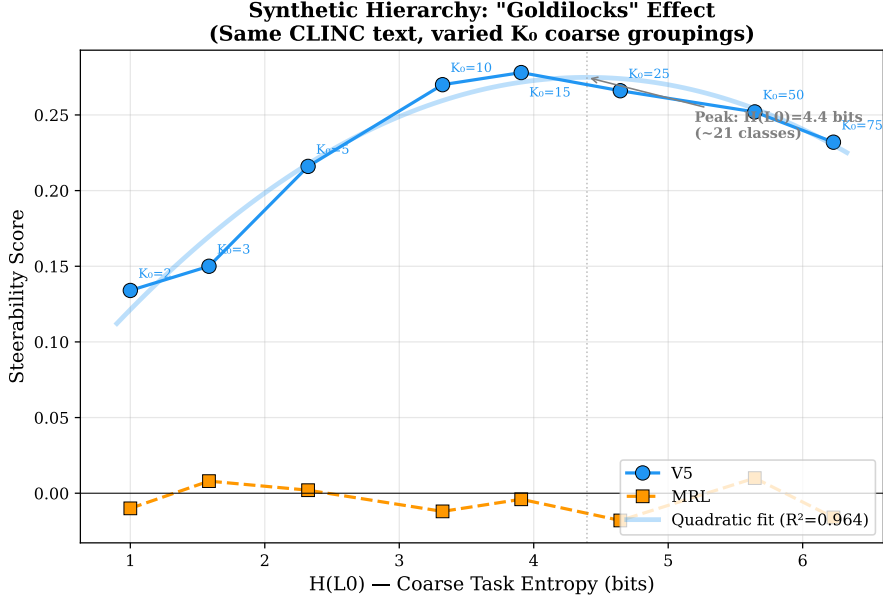


Figure 5: Synthetic hierarchy experiment: steerability peaks when coarse entropy $H(L_0)$ matches prefix capacity ($K_0 \approx 12\text{--}16$), revealing a Goldilocks effect. Quadratic $R^2 = 0.964$. MRL stays near zero throughout.

is the *unfinetuned* baseline L_1 accuracy—a measure of how much fine-grained information the pre-trained backbone captures before any training:

- $H(L_1|L_0)$ alone: $\rho = 0.74$ ($p = 0.035$)
- $A_{L_1}^{\text{base}}$ alone: $\rho = 0.69$ ($p = 0.058$)
- $H(L_1|L_0) \times A_{L_1}^{\text{base}}$: $\rho = 0.90$ ($p = 0.002$); Pearson $r = 0.97$ ($p < 0.001$)

The product predictor correctly places WOS among lower-steerability datasets: it has the highest $H(L_1|L_0)$ but the lowest $A_{L_1}^{\text{base}}$ (17.0%, vs. 88.7% for CLINC). A leave-one-out analysis confirms robustness: all LOO $\rho \geq 0.61$, and bootstrap 95% CI for $\rho(H(L_1|L_0))$ is $[0.05, 1.0]$ with 98.0% positive (Appendix K).

6.2 Causal: Synthetic Hierarchy Experiment

Natural datasets confound $H(L_0)$ (prefix task demand) with $H(L_1|L_0)$ (refinement complexity), since more coarse classes typically yield more fine subclasses. To disentangle these, we construct synthetic hierarchies on CLINC-150 text with fixed total entropy $H(L_1) = \log_2 150$ but varying coarse partitions $K_0 \in \{2, 3, 5, 10, 15, 25, 50, 75\}$.

The Goldilocks effect. Figure 5 and Table 5 reveal an inverted-U relationship:

1. **Rising phase** ($K_0 = 2 \rightarrow 15$): more coarse classes create a richer “routing codebook” for the 64d prefix, enabling finer coarse discrimination.
2. **Falling phase** ($K_0 = 15 \rightarrow 75$): $H(L_0)$ exceeds the prefix’s representational capacity. With 64 dimensions, the prefix cannot reliably distinguish 50+ coarse classes.
3. **Optimum:** peak at $K_0 \approx 12\text{--}16$ ($H^*(L_0) \approx 3.6\text{--}4.0$ bits), matching the effective capacity of a 64-dimensional prefix. A quadratic fit captures the shape with $R^2 = 0.964$.
4. **MRL control:** MRL steerability remains near zero ($|\mathcal{S}| < 0.02$) across all conditions, confirming the requirement for hierarchy-aligned supervision.

Table 5: Synthetic hierarchy experiment. Fixed total entropy ($\log_2 150 = 7.23$ bits), varying K_0 . Steerability peaks at $K_0 \approx 15$ —a capacity–demand matching optimum.

K_0	$H(L_0)$	$H(L_1 L_0)$	Branch	V5 \mathcal{S}	MRL \mathcal{S}	Gap
2	1.00	6.23	75.0	+0.134	-0.010	+0.144
3	1.58	5.64	50.0	+0.150	+0.008	+0.142
5	2.32	4.90	30.0	+0.216	+0.002	+0.214
10	3.32	3.90	15.0	+0.270	-0.012	+0.282
15	3.91	3.32	10.0	+0.278	-0.004	+0.282
25	4.64	2.58	6.0	+0.266	-0.018	+0.284
50	5.64	1.58	3.0	+0.252	+0.010	+0.242
75	6.23	1.00	2.0	+0.232	-0.016	+0.248

Table 6: Cross-model replication (3 seeds each). Steerability is architecture-invariant across three encoder families ($p < 0.025$, Holm-corrected, $m = 3$).

Model	CLINC ($H(L_1 L_0) = 3.90$)		TREC ($H(L_1 L_0) = 2.21$)	
	V5 \mathcal{S}	MRL \mathcal{S}	V5 \mathcal{S}	MRL \mathcal{S}
BGE-small (BAAI, 33M)	+0.150 ± 0.028	+0.007 ± 0.016	+0.044 ± 0.017	-0.001 ± 0.015
E5-small (Microsoft, 33M)	+0.130 ± 0.031	+0.015 ± 0.008	—	—
Qwen3-0.6B (Alibaba, 600M)	+0.153 ± 0.013	+0.008 ± 0.006	+0.081 ± 0.012	+0.011 ± 0.002

The synthetic experiment also resolves the observational confound: steerability is driven by $H(L_0)$ (prefix task demand), not $H(L_1|L_0)$. In natural datasets, the $H(L_1|L_0)$ correlation arises because the two entropies covary. Figure 6 in the appendix visualises both relationships.

7 Generality, Downstream Utility, and Extensions

Cross-model replication. We replicate the CLINC experiment on E5-small-v2 (Microsoft, contrastive pre-training, 384d) and Qwen3-Embedding-0.6B ($h = 1024$, 18× more parameters). Table 6 confirms that the steerability gap is architecture-invariant: BGE-small +0.144, E5-small +0.130, Qwen3 +0.153 (all $p < 0.025$, Holm-corrected across 3 families). MRL steerability remains ≤ 0.015 on all models. The larger Qwen3 backbone shows higher steerability, suggesting the effect scales with model capacity.

Downstream retrieval. We evaluate whether steerability transfers beyond classification to controllable retrieval. Table 7 reports Recall@1 on CLINC at each prefix length (3 seeds; full ramp in Figure 7, Appendix). V5 L_1 Recall@1 climbs from 87.1% (64d) to 93.4% (256d)—a +6.3pp ramp, 10× larger than MRL’s +0.6pp. This demonstrates that prefix-level semantic specialisation directly yields dimensionality-dependent retrieval resolution.

Workload-adaptive Pareto advantage. V5’s steerability enables query-adaptive routing: coarse queries use the 64d prefix, fine queries use the full 256d embedding. On CLINC (5 seeds), this dominates MRL-256d whenever $\geq 35\%$ of queries are coarse. At a 50/50 workload mix, V5 adaptive achieves +1.3pp higher accuracy at 38% lower average dimensionality (160d vs. 256d). The dimensionality savings translate to wall-clock speedups: on FAISS HNSW indexes with 100K vectors, 64d queries execute 3.7× faster than 256d (39 μ s vs. 145 μ s; Table 9, Appendix).

Single model replaces two. A natural alternative to V5 is training two dedicated encoders: E_{L_0} for coarse and E_{L_1} for fine, each at 256d. On CLINC (3 seeds), the dual system achieves $L_0 = 95.8\%$ and $L_1 = 94.8\%$, requiring two models and two indexes. V5 adaptive (64d for coarse, 256d for fine) achieves $L_0 = 97.5\%$ at one-quarter the dimensionality and $L_1 = 94.5\%$ at full resolution—*higher* coarse accuracy from a single model.

Three-level hierarchy. To test generalisation beyond two levels, we construct a 3-level CLINC hierarchy: 5 super-domains → 10 domains → 150 intents. V5 exhibits a clear ramp gradient: L_2 (intent) accuracy gains +3.2pp from 64d to 256d, L_1 (domain) gains +1.0pp, and L_0 (super-domain)

Table 7: Retrieval Recall@1 on CLINC-150 (3 seeds). V5’s L_1 ramp (+6.3pp) is $10\times$ MRL’s (+0.6pp).

Level	Method	Recall@1 (%)			
		64d	128d	192d	256d
L_0	V5	97.2	97.8	98.0	97.9
	MRL	97.7	98.0	98.2	98.1
L_1	V5	87.1	92.7	93.7	93.4
	MRL	93.6	93.9	94.3	94.3
L_1 ramp (256d–64d)		V5: +6.3 ± 0.9pp		MRL: +0.6 ± 0.3pp	
				Ratio: 10×	

Table 8: Three-level hierarchy (CLINC, 5→10→150, 3 seeds). V5 shows a ramp gradient: finer levels gain more from additional dimensions. MRL is flat.

Level	Method	k-NN Accuracy (%)			
		64d	128d	192d	256d
L_0 (5 super)	V5	98.6	98.9	99.0	99.1
	MRL	98.4	98.6	98.6	98.7
L_1 (10 domain)	V5	97.7	98.3	98.5	98.7
	MRL	97.9	98.0	98.1	98.1
L_2 (150 intent)	V5	92.7	94.7	95.4	95.9
	MRL	94.9	95.2	95.3	95.3

gains +0.5pp. MRL is flat at all levels (≤ 0.4 pp; Table 8). Three-level steerability $S_{02} = +0.027 \pm 0.005$ (V5) vs. $+0.002 \pm 0.005$ (MRL; $t = 18.9$, $p = 0.003$, $d = 10.9$).

8 Limitations

- **Shallow hierarchies.** On datasets with low $H(L_1|L_0)$ (e.g., Yahoo, $H(L_1|L_0) = 1.23$), steerability is small and noisy ($S = 0.015 \pm 0.019$). The method is most valuable for moderately deep hierarchies where the fine task is learnable.
- **Floor effects.** On WOS ($K_1 = 336$), head-only training achieves only $\sim 15\%$ L_1 accuracy, capping steerability despite high $H(L_1|L_0) = 5.05$. Steerability requires both hierarchy complexity and model capacity.
- **Deeper hierarchies.** The 3-level extension confirms generalisation with a strong effect ($d = 10.9$), but only 5 super-domain classes leave L_0 near ceiling at all prefixes. Evaluation on naturally deep taxonomies (ICD-10, product hierarchies) remains future work.
- **Hierarchy noise robustness.** Corrupting L_0 labels at 10%–50% and retraining V5 on CLINC (3 seeds), steerability degrades gracefully: 85% retained at 10% noise ($S = +0.152$), 71% at 30% (+0.128), 34% at 50% (+0.061). V5 does not require a perfect hierarchy for meaningful steerability.
- **Baseline scope.** We compare against a matched MRL baseline controlling all variables except the prefix-to-label mapping. We do not benchmark HEAL [Bhattarai et al., 2025], CSR [Wen et al., 2025], or SMRL [Zhang et al., 2025] because these address orthogonal goals—none offers prefix-level steering, making fixed-dimensionality accuracy comparisons inapposite.
- **Ablation coverage.** Causal ablations are concentrated on CLINC and TREC (two datasets). Cross-dataset replication of all four ablation conditions remains future work.

9 Theoretical Analysis: Successive Refinement

We connect our empirical findings to the classical theory of *successive refinement* [Equitz and Cover, 1991, Rimoldi, 1994], providing formal conditions for when and why hierarchy-aligned supervision produces steerability.

Setup. Let (X, Y_0, Y_1) be a hierarchical source with $Y_0 = g(Y_1)$. An encoder produces $\mathbf{z} = [\mathbf{z}_1; \dots; \mathbf{z}_J] \in \mathbb{R}^d$ with prefix $\mathbf{z}_{\leq m} = [\mathbf{z}_1; \dots; \mathbf{z}_m]$. Let $C(d')$ denote the effective capacity (in bits) of a d' -dimensional embedding.

Theorem 1 (Hierarchy-Successive-Refinement, informal). Assume $C(d/J) \geq H(L_0)$ and $C(d/J) < H(L_1)$. Under V5 supervision ($\mathbf{z}_{\leq 1} \rightarrow L_0$, $\mathbf{z} \rightarrow L_1$):

$$I(\mathbf{z}_{\leq 1}; L_0) > I(\mathbf{z}_{\leq 1}; L_1 | L_0) \quad (\text{coarse-prioritised prefix}) \quad (5)$$

Under MRL ($\mathbf{z}_{\leq 1} \rightarrow L_1$, $\mathbf{z} \rightarrow L_1$): no specialisation.

The proof follows from the capacity bottleneck: V5’s prefix loss targets only L_0 , so the optimal prefix maximises $I(\mathbf{z}_{\leq 1}; L_0)$. Since $C(d/J) < H(L_1)$ but $C(d/J) \geq H(L_0)$, the prefix allocates capacity preferentially to the coarse task. MRL distributes capacity across both L_0 and $L_1 | L_0$ without specialisation.

Connection to successive refinement. Hierarchical sources are naturally *successively refinable* [Rimoldi, 1994]: the optimal multi-resolution code first encodes Y_0 at rate $R_1 \geq H(Y_0)$, then encodes the residual $Y_1 | Y_0$ at rate $R_2 \geq H(Y_1 | Y_0)$. V5 approximates this structure: block 1 encodes Y_0 ; blocks 2–J encode the refinement. MRL performs single-resolution coding at each rate, losing the nested structure. This explains why V5 achieves accuracy parity at full resolution while gaining steerability at short prefixes.

The successive refinement framework yields three testable predictions, all confirmed:

Corollary 1 (Sign reversal). Under inverted supervision ($\mathbf{z}_{\leq 1} \rightarrow L_1$, $\mathbf{z} \rightarrow L_0$), the bottleneck forces the prefix to encode refinement information, producing $\mathcal{S} < 0$. Confirmed: $\mathcal{S} = -0.018$ (CLINC), -0.025 (TREC).

Corollary 2 (UHMT collapse). Under uniform multi-task supervision, no prefix is privileged for either task; the optimiser distributes information uniformly, yielding $\mathcal{S} \approx 0$. Confirmed: $\mathcal{S} = +0.001$ (CLINC), -0.009 (TREC).

Theorem 2 (Goldilocks capacity-demand matching, informal). With fixed $H(Y_1)$ and varying K_0 , steerability peaks at $H^*(L_0) \approx C(d/J)$:

- $H(L_0) < C(d/J)$: spare capacity leaks $L_1 | L_0$ information, reducing \mathcal{S} .
- $H(L_0) > C(d/J)$: by Fano’s inequality, prefix errors degrade coarse classification, reducing \mathcal{S} .
- *Taylor expansion around H^* :* $\mathcal{S} \approx \mathcal{S}^* - \alpha(H(L_0) - H^*)^2$, matching the empirical quadratic fit ($R^2 = 0.964$).

Testable prediction. Doubling prefix capacity from 64 to 128 dimensions should shift the Goldilocks peak rightward (to higher K_0), verifiable via a capacity sweep.

10 Related Work

Multi-resolution embeddings. MRL [Kusupati et al., 2022] trains embeddings supporting prefix truncation, but all lengths target the same task. SMEC [Zhang et al., 2025] rethinks MRL training for retrieval compression; Matryoshka Multimodal Models [Cai et al., 2025] apply the nesting principle to visual tokens. Most closely related, Hanley and Durumeric [2025] independently train multilingual Matryoshka embeddings where different dimension subsets capture story similarity at different granularity levels for news clustering. Our work provides complementary contributions: a

formal successive-refinement framework, an explicit steerability metric with causal ablations, evaluation across eight domains and three encoder families, and a scaling trend linking steerability to hierarchy structure.

Dimensional redundancy. Dufter et al. [2025] show that randomly removing 50% of dimensions causes <10% performance loss, revealing massive redundancy. We exploit this differently: rather than discarding dimensions for compression, we *structure* them to carry semantically distinct information at each prefix length. Luan et al. [2025] prove that single-vector embedding expressiveness for top- k retrieval is bounded by dimensionality, motivating multi-resolution access patterns.

Hierarchical embeddings. Hyperbolic embeddings [Nickel and Kiela, 2017] represent hierarchies through curved geometry. HEAL [Bhattarai et al., 2025] aligns LLM embeddings with domain hierarchies via contrastive losses and matrix factorisation, but does not offer steerability via dimensional truncation.

Sparse and compressed embeddings. CSR [Wen et al., 2025] and CSRV2 [Guo et al., 2026] learn sparse codes as alternatives to MRL, achieving efficiency through selective activation. These address adaptive dimensionality via sparsity; our approach uses hierarchical prefix structure. The two are orthogonal and potentially complementary.

11 Conclusion

We have shown that aligning prefix supervision with semantic hierarchy converts dimensional truncation from a fidelity knob into a *semantic zoom* control—at zero inference cost. The evidence is threefold. *Empirically*, fractal training produces steerability on all eight datasets (pooled $d = 1.49$, $p = 0.0003$), with magnitude predicted by the product of hierarchy depth and baseline learnability ($\rho = 0.90$). *Causally*, four controlled ablations on two datasets establish that the specific prefix-to-hierarchy alignment—not hierarchy awareness, not architecture, not optimiser—drives the effect; sign reversal under inversion and collapse under uniform multi-task training both replicate. *Theoretically*, the successive refinement framework explains *why* V5 works (capacity bottleneck forces coarse-first encoding) and *when* it works best (Goldilocks capacity–demand matching, $R^2 = 0.964$).

The practical implications are concrete. A single fractal embedding enables query-adaptive retrieval: routing coarse queries to the 64d prefix ($3.7 \times$ faster on HNSW) and fine queries to 256d, yielding higher mixed accuracy than MRL at 38% lower compute. A single V5 model replaces a dual-encoder system: its 64d prefix achieves 97.5% coarse accuracy, exceeding a dedicated 256d coarse encoder (95.8%). The synthetic hierarchy experiment provides design guidance: measure $H(L_0)$ and size prefix capacity to match.

The connection to successive refinement suggests this is not an empirical curiosity but a fundamental property of information allocation in hierarchical representations. We release all code, data, and experimental artifacts to support replication and extension.

References

- Manish Bhattarai, Ryan Barron, Maksim E. Eren, Minh N. Vu, Vesselin Grantcharov, Ismael Boureima, Valentin Stanev, Cynthia Matuszek, Vladimir I. Valtchinov, Kim Rasmussen, and Boian S. Alexandrov. HEAL: Hierarchical embedding alignment loss for improved retrieval and representation learning. In *International Conference on Learning Representations*, 2025.
- Mu Cai et al. Matryoshka multimodal models. In *International Conference on Learning Representations*, 2025.
- Colin B Clement, Matthew Biber, Kelly F Thomson, and Arvind Sundaram. On the use of arxiv as a dataset. In *NeurIPS Workshop on Machine Learning for Creativity and Design*, 2019.
- Dorottya Demszky, Dana Movshovitz-Attias, Jeongwoo Ko, Alan Cowen, Gaurav Nemade, and Sujith Ravi. Goemotions: A dataset of fine-grained emotions. In *Proceedings of the 58th Annual Meeting of the Association for Computational Linguistics*, pages 4040–4054, 2020.

Philipp Dufter et al. Randomly removing 50% of dimensions in text embeddings has minimal impact. *arXiv preprint arXiv:2508.17744*, 2025.

William H R Equitz and Thomas M Cover. Successive refinement of information. *IEEE Transactions on Information Theory*, 37(2):269–275, 1991.

Lixuan Guo, Yifei Wang, Tiansheng Wen, Yifan Wang, Aosong Feng, Bo Chen, Stefanie Jegelka, and Chenyu You. CSRV2: Unlocking ultra-sparse embeddings. In *International Conference on Learning Representations*, 2026.

Hans W. A. Hanley and Zakir Durumeric. Hierarchical level-wise news article clustering via multi-lingual matryoshka embeddings. In *Proceedings of the 63rd Annual Meeting of the Association for Computational Linguistics (Volume 1: Long Papers)*, pages 2476–2492, 2025.

Sture Holm. A simple sequentially rejective multiple test procedure. *Scandinavian Journal of Statistics*, 6(2):65–70, 1979.

Kamran Kowsari, Donald E. Brown, Mojtaba Heidarysafa, Kiana Jafari Meimandi, Matthew S. Gerber, and Laura E. Barnes. HDLTex: Hierarchical deep learning for text classification. In *IEEE International Conference on Machine Learning and Applications*, 2017.

Aditya Kusupati, Gantavya Bhatt, Aniket Rege, Matthew Wallingford, Aditya Sinha, Vivek Ramanujan, William Howard-Snyder, Kaifeng Chen, Sham Kakade, Prateek Jain, and Ali Farhadi. Matryoshka representation learning. In *Advances in Neural Information Processing Systems*, 2022.

Stefan Larson, Anish Mahendran, Joseph J Peper, Christopher Clarke, Andrew Lee, Parker Hill, Jonathan K Kummerfeld, Kevin Leach, Michael A Laurenzano, Lingjia Tang, and Jason Mars. An evaluation dataset for intent classification and out-of-scope prediction. *Proceedings of the Conference on Empirical Methods in Natural Language Processing*, 2019.

Yi Luan et al. On the theoretical limitations of embedding-based retrieval. *arXiv preprint arXiv:2508.21038*, 2025.

Maximilian Nickel and Douwe Kiela. Poincaré embeddings for learning hierarchical representations. In *Advances in Neural Information Processing Systems*, 2017.

Béat Rimoldi. Successive refinement of information: Characterization of the achievable rates. *IEEE Transactions on Information Theory*, 40(1):253–259, 1994.

Ellen M Voorhees and Dawn M Tice. Building a question answering test collection. *Proceedings of the ACM SIGIR Conference*, 2000.

Tiansheng Wen, Yifei Wang, Zequn Zeng, Zhong Peng, Yudi Su, Xinyang Liu, Bo Chen, Hongwei Liu, Stefanie Jegelka, and Chenyu You. Beyond matryoshka: Revisiting sparse coding for adaptive representation. In *Proceedings of the International Conference on Machine Learning*, 2025.

Shitao Xiao, Zheng Liu, Peitian Zhang, and Niklas Muennighoff. C-pack: Packaged resources to advance general chinese embedding. *arXiv preprint arXiv:2309.07597*, 2023.

Biao Zhang, Lixin Chen, Tong Liu, and Bo Zheng. SMEC: Rethinking matryoshka representation learning for retrieval embedding compression. In *Proceedings of the Conference on Empirical Methods in Natural Language Processing*, 2025.

Xiang Zhang, Junbo Zhao, and Yann LeCun. Character-level convolutional networks for text classification. *Advances in Neural Information Processing Systems*, 2015.

Disentangling the Scaling Law: $H(L_0)$ is the True Driver

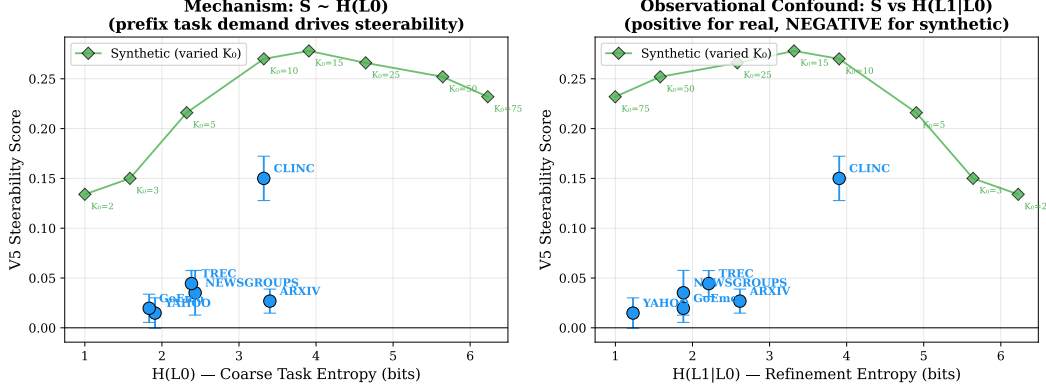


Figure 6: Disentangling the scaling law. **Left:** Steerability vs. $H(L_0)$ (prefix task demand)—the true driver, confirmed by the synthetic experiment. **Right:** Steerability vs. $H(L_1|L_0)$ —a confounded proxy in observational data. Synthetic data (green diamonds) breaks the confound: $H(L_1|L_0)$ anti-correlates with steerability when $H(L_0)$ is varied independently.

Retrieval Benchmark: V5 Enables Coarse-to-Fine Recall via Truncation

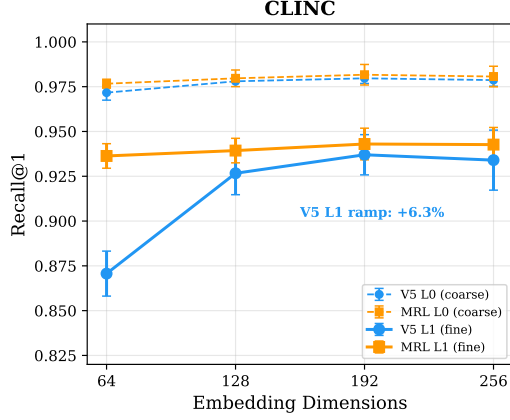


Figure 7: Retrieval benchmark on CLINC-150 (3 seeds). V5 L_1 Recall@1 ramps steeply from 64d to 192d (+6.3pp) while MRL is flat (+0.6pp). Both achieve comparable L_0 Recall@1 (> 97%). The 10 \times larger ramp demonstrates that prefix specialisation transfers from classification to retrieval.

3-Level Hierarchy: Monotonic Semantic Zoom (CLINC 5->10->150)

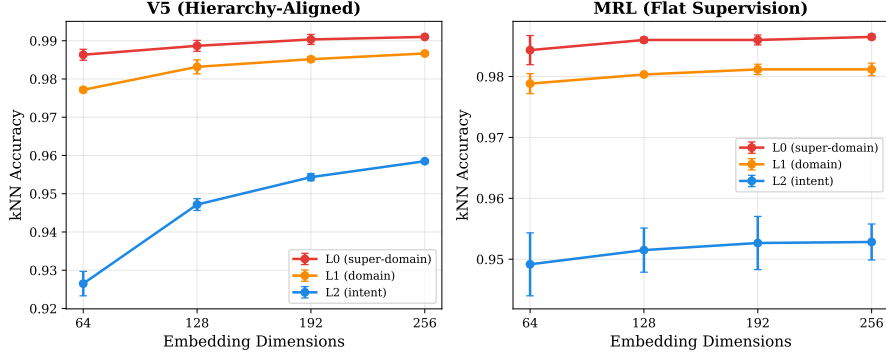


Figure 8: Three-level hierarchy (CLINC, 5->10->150, 3 seeds). **Left:** V5 shows clear level separation— L_2 gains most from additional dimensions while L_0 is near ceiling. **Right:** MRL curves are bunched with minimal ramp at any level.

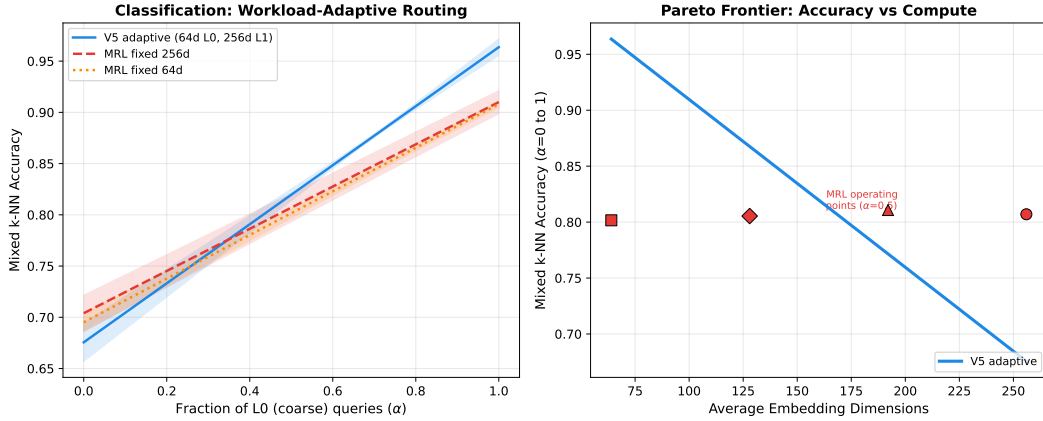


Figure 9: **Left:** Mixed accuracy vs. workload mix α (fraction coarse). V5 adaptive dominates MRL-256d for $\alpha \geq 0.35$. **Right:** Pareto frontier—V5 achieves higher accuracy at lower dimensionality. Bands: ± 1 SD (5 seeds).

A Entropy Allocation Analysis

B Retrieval Benchmark Visualisation

C Three-Level Hierarchy Visualisation

D Workload-Adaptive Pareto Analysis

E FAISS Latency Benchmark

F Full Synthetic Hierarchy Results

See Table 5 for complete results across all 8 coarse partition sizes. The experiment holds total class count fixed at 150 while varying K_0 from 2 to 75 with randomly assigned hierarchies on CLINC-150 text.

Table 9: FAISS query latency at different dimensionalities (RTX 5090, float32). V5’s 64d prefix queries are 3.7–5.1× faster than 256d.

Dim	Flat (n=10K)		HNSW (n=100K)	
	Latency (μ s)	Speedup	Latency (μ s)	Speedup
64d	35	5.1×	39	3.7×
128d	110	1.6×	87	1.7×
192d	146	1.2×	81	1.8×
256d	179	1.0×	145	1.0×

G Training Convergence

All models converge within 5 epochs of head-only training. Stage 2 (backbone fine-tuning) was tested but provided no improvement, consistent with the frozen backbone providing sufficient representational capacity for hierarchy-aligned supervision.

H Reproducibility

Code and data. All code, trained models, and result JSONs are available at <https://github.com/dl1683/ai-moonshots>. Every experiment uses publicly available datasets loaded via the `datasets` library with deterministic seeded splits.

Hyperparameters. All experiments use: 5 epochs head-only training, batch size 16, lr 10^{-4} , AdamW with cosine decay, FP16, gradient clipping at 1.0. Prefix sampling [0.4, 0.3, 0.2, 0.1] and block dropout [0.95, 0.9, 0.8, 0.7] are fixed across all datasets and models. No per-dataset tuning.

Compute. Single NVIDIA RTX 5090 Laptop GPU (24GB VRAM). Each training run: ~2 min (BGE-small, 33M) or ~8 min (Qwen3-0.6B). Full suite: ~16 GPU-hours.

I Metric Robustness

We verify conclusions hold under three alternative steerability formulations:

- \mathcal{S}_{AUC} : average steerability over all prefix pairs $k = 2, 3, 4$.
- $\mathcal{S}_{\text{mono}}$: fraction of adjacent pairs with monotonic coarse-decrease / fine-increase.
- \mathcal{S}_{gap} : specialisation gap $(L_0 @ j_1 - L_1 @ j_1) - (L_0 @ j_4 - L_1 @ j_4)$.

Table 10: Metric robustness: V5 – MRL gap under four steerability formulations. Three of four agree V5 > MRL on all 8 datasets.

Dataset	$H(L_1 L_0)$	$\Delta \mathcal{S}_{\text{orig}}$	$\Delta \mathcal{S}_{\text{AUC}}$	$\Delta \mathcal{S}_{\text{mono}}$	$\Delta \mathcal{S}_{\text{gap}}$
Yahoo	1.23	+0.010	+0.013	-0.10	+0.010
GoEmotions	1.88	+0.014	+0.014	-0.07	+0.014
Newsgroups	1.88	+0.035	+0.037	+0.03	+0.035
TREC	2.21	+0.045	+0.039	+0.27	+0.045
arXiv	2.62	+0.028	+0.020	+0.17	+0.028
DBpedia Cl.	3.17	+0.112	+0.106	+0.33	+0.112
CLINC	3.90	+0.143	+0.124	+0.27	+0.143
WOS	5.05	+0.036	+0.027	+0.30	+0.036
V5 > MRL		8/8	8/8	6/8	8/8
Sign test p		0.004	0.004	0.14	0.004

All pairwise rank correlations exceed $\rho = 0.90$ ($p < 0.005$), confirming all four metrics recover the same dataset ordering.

J Per-Seed Steerability Values

Table 11: Per-seed steerability (V5 and MRL) across all eight datasets. Seeds: 42, 123, 456, 789, 1024.

Dataset	V5 \mathcal{S} by seed					MRL \mathcal{S} by seed				
	42	123	456	789	1024	42	123	456	789	1024
Yahoo	+.016	+.020	-.004	-.002	+.044	-.010	+.016	+.006	+.016	-.002
GoEmo	-.002	+.024	+.026	+.006	+.044	+.022	+.022	+.006	-.012	-.010
News	+.040	-.012	+.038	+.044	+.066	-.002	+.022	+.008	-.018	-.010
TREC	+.018	+.062	+.054	+.042	+.046	+.000	+.024	-.014	-.002	-.012
arXiv	+.038	+.018	+.012	+.018	+.048	-.014	-.010	+.000	+.000	+.020
DBP	+.118	+.092	+.130	+.130	+.130	+.020	+.008	+.008	+.000	+.002
CLINC	+.104	+.178	+.150	+.168	+.150	+.012	+.028	+.006	-.016	+.004
WOS	+.032	+.022	+.008	+.052	+.074	+.000	-.004	+.004	-.004	+.010

K Scaling Trend Robustness

Table 12: Leave-one-out sensitivity for the $H(L_1|L_0)$ scaling trend. WOS (Cook’s $D = 3.68$) is the highest-influence point; the product predictor resolves its deviation without dropping any dataset.

Dropped	k	Spearman ρ	p	Pearson r	p
None (full)	8	0.74	0.035	0.49	0.218
Yahoo	7	0.61	0.144	0.40	0.376
GoEmotions	7	0.64	0.119	0.45	0.318
Newsgroups	7	0.71	0.071	0.47	0.289
TREC	7	0.83	0.021	0.48	0.272
arXiv	7	0.78	0.041	0.50	0.259
DBpedia Classes	7	0.72	0.068	0.49	0.261
CLINC	7	0.72	0.068	0.34	0.457
WOS	7	0.87	0.012	0.91	0.004

Bootstrap analysis (10,000 resamples): 98.0% of $\rho(H(L_1|L_0))$ values positive. Meta-analysis prediction interval $[-0.70, 3.18]$ reflects heterogeneity ($I^2 = 63\%$) explained by the interaction model.

L Broader Impact

Fractal embeddings add a semantic control knob to existing embedding models without modifying the backbone. The primary application is more efficient retrieval: coarse-first filtering reduces compute by $4\times$ without sacrificing fine-grained accuracy when needed. We do not foresee negative societal impacts beyond those inherent to embedding-based retrieval generally. The method is domain-agnostic and introduces no biases beyond those present in the frozen backbone.